Wave propagation analyses considering an enhanced fully adaptive explicit time-marching formulation

Lucas Ruffo Pinto[1], Delfim Soares Jr.[2], Webe João Mansur[1]

[1]*COPPE/Federal University of Rio de Janeiro*
CEP 21941-611, Rio de Janeiro, Brazil
lucas.ruffo@engenharia.ufjf.br, webe@coc.ufrj.br
[2]*Structural Engineering Department, Federal University of Juiz de Fora*
CEP 36036-330, Juiz de Fora, MG, Brazil
delfim.soares@ufjf.edu.br

Abstract. This work presents an enhanced explicit time-marching formulation to analyse hyperbolic models, which is based on locally-defined adaptive time-integrators and time-step values. The discussed technique considers single-step displacement/velocity recurrence relations, providing an easy to implement, truly self-starting methodology. The stability limit of the approach is twice that of the central difference method, and it allows adaptive controllable numerical dissipation to be applied, improving the accuracy and versatility of the method. As an explicit approach, the technique does not require the solution of any system of equations, standing as a very efficient methodology. Subdomain decomposition procedures, associated to multiple time-step values and sub-cycling, are also considered, improving the performance and accuracy of the technique. The entire formulation is carried out taking into account automated, self-adjustable computations, requiring no effort and/or expertise from the user. At the end of the paper, numerical results are presented and compared to those of standard techniques, illustrating the great effectiveness of the discussed approach.

Keywords: Time-marching, Explicit analysis, Adaptive parameters.

1 Introduction

Time-dependent hyperbolic equations have numerous applications in geophysics, as they make it possible to describe time-dependent continuous domain physical problems. However, their analytical resolution is often unfeasible, thereby, numerical methods are commonly used to find approximate solutions. Time domain solution algorithms usually employ step-by-step time integration procedures, solving initial value problems considering a temporal discretization. Numerical methods are basically divided into two groups: explicit methods [1-9], whose main advantage is that there is no need to deal with algorithms for solving systems of equations, making them computationally effective, yet with stability restrictions; and implicit methods [9-15], which usually provide unconditional stability, but are considerably more computationally expensive per time step (for a comprehensive review, see [16]).

In this paper, an explicit formulation with adaptive time integrators developed by Soares [1] is studied, considering the implementation of subcycling techniques to improve the efficiency and accuracy of the proposed time integration algorithm. This method is based on single-step displacement-velocity relationships; it is truly self-starting; provides twice the stability limit of the central differences method (CDM); and, as an explicit approach, it does not need to consider any solver routines. In this work, as a further development for this solution procedure, subdomain splits and local time-step values are considered, taking into account also automated adaptive evaluations. Thus, more efficient and accurate analyses can be enabled.

The adopted time integration procedure is based on adaptive parameters that aim to provide numerically efficientedissipative algorithms, aiming to eliminate the influence of spurious high frequency modes and reduce amplitude decay errors. In this sense, a time integrator β is adaptively calculated taking into account the maximum

sampling frequency of the elements and the value of the local time-step. In addition, the adaptive parameters are activated considering the results of the previous local time steps. Thus, by introducing different time-steps in the analysis (considering subdomain divisions and subcycling techniques), the performance of the methodology can be improved.

The technique discussed in this work can be used to solve problems of different natures, however, here, acoustic analyses and geophysical applications are focused. In geophysics, it is routinely necessary to analyze heterogeneous domains, characterized by multiple layers of fine stratigraphy and distinct geometries. In this sense, automatic subcycling techniques become very attractive, since different layers/media can be efficiently analyzed considering the appropriate subdomain divisions.

This article is divided into five sections, the first being this introduction. In the second section, the equations that govern the time integration strategy are presented. In the third section, a generic automatic methodology for sub-cycling is discussed. In the fourth section, two numerical applications are considered, illustrating the good performance of the proposed technique (in this case, the obtained results are compared to those of the CDM and of the explicit generalized α method (EG-α) [8], as well as with analytical solutions, whenever available). In the fifth and final section, conclusions are presented.

2 Governing equations and time integration strategy

The governing system of equations describing a dynamic model is given by:

$$\mathbf{M}\ddot{\mathbf{U}}(\mathrm{t}) + \mathbf{C}\dot{\mathbf{U}}(\mathrm{t}) + \mathbf{K}\mathbf{U}(\mathrm{t}) = \mathbf{F}(\mathrm{t}), \tag{1}$$

where $\mathbf{M}$, $\mathbf{C}$, and $\mathbf{K}$ stand for the mass, damping, and stiffness matrices, respectively; $\ddot{\mathbf{U}}(\mathrm{t})$, $\dot{\mathbf{U}}(\mathrm{t})$ and $\mathbf{U}(\mathrm{t})$ are acceleration, velocity, and displacement vectors, respectively; and $\mathbf{F}(\mathrm{t})$ stands for the force vector. The initial conditions of the model are given by: $\mathbf{U}^0 = \mathbf{U}(0)$ and $\dot{\mathbf{U}}^0 = \dot{\mathbf{U}}(0)$, where $\mathbf{U}^0$ and $\dot{\mathbf{U}}^0$ stand for initial displacement and velocity vectors, respectively.

In this work, the standard Finite Element Method (FEM) is used for the spatial discretization where the domain of the problem is divided into elements, allowing the calculation of local matrices and vectors, which can then be assembled to generate the global matrices $\mathbf{M}$, $\mathbf{C}$ and $\mathbf{K}$, and vector $\mathbf{F}$.

For the time-domain solution of the system of equations (1), the following algorithm is proposed by Soares [1]:

$$\left(\boldsymbol{M} + \frac{1}{2}\Delta t\boldsymbol{C}\right)\dot{\boldsymbol{U}}^{n+1} = \int_{t^n}^{t^{n+1}} \boldsymbol{F}(t)\,dt + \boldsymbol{M}\dot{\boldsymbol{U}}^n - \frac{1}{2}\Delta t\boldsymbol{C}\dot{\boldsymbol{U}}^n - \Delta t\boldsymbol{K}\left(\boldsymbol{U}^n + \frac{1}{2}\Delta t\dot{\boldsymbol{U}}^n\right), \tag{2a}$$

$$\boldsymbol{U}^{n+1} = \boldsymbol{U}^n + \frac{1}{2}\Delta t\dot{\boldsymbol{U}}^n + \frac{1}{2}\Delta t\dot{\boldsymbol{U}}^{n+1} + \frac{1}{2}\Delta t\boldsymbol{V}^{n+1}, \tag{2b}$$

where a $\mathbf{V}^{n+1}$ term is considered in equation (2b), allowing to obtain greater stability limits for the explicit analysis. The vector $\mathbf{V}^{n+1}$ is computed as follows:

$$\left(\boldsymbol{M}_e + \frac{1}{2}\Delta t\boldsymbol{C}_e\right)\boldsymbol{V}_e^{n+1} = -\Delta t\boldsymbol{C}_e\dot{\boldsymbol{U}}_e^{n+1} - \frac{1}{8}\Delta t^2\boldsymbol{K}_e\left((\beta_e^n)^2\dot{\boldsymbol{U}}_e^n + (1+\beta_e^n)\dot{\boldsymbol{U}}_e^{n+1}\right). \tag{3}$$

As can be seen, in the proposed new formulation, the temporal integration parameter of the method is spatially and temporally locally defined, as indicated by the sub and superscripts of β_e^n. Thereby, different values can be assigned to the time integrator, for each element of the model and for each time step of the analysis, providing a very flexible approach. Thus, a spatial/temporal adaptive procedure may be developed, locally computing the time integration parameter β_e^n according to the properties of the model and to the evolution of the computed fields.

The strategy here is to adopt $\beta_e^n > 0$ whenever and wherever numerical damping may be necessary, and $\beta_e^n = 0$ otherwise. This can be automatically carried out based on an oscillatory criterion. In this sense, if the computed response of a degree of freedom of the model oscillates along time, the β_e^n parameters of the elements surrounding this degree of freedom are modified, locally introducing numerical dissipation into the analysis. Once no oscillatory behaviour is observed, $\beta_e^n = 0$ is considered. This is automatically carried out here based on an oscillatory criterion controlled by a φ parameter, that is calculated at each time step and for each element. The calculation of this oscillatory parameter is given by: $\varphi_e^n = \Sigma_{i=1}^{d_e}\left|\left|u_i^n - u_i^{n-2}\right| - \left|u_i^n - u_i^{n-1}\right| - \left|u_i^{n-1} - u_i^{n-2}\right|\right|$,

where d_e stands for the total amount of degrees of freedom of the element. Therefore, when $\varphi \neq 0$, at least one degree of freedom of the element is oscillating. Thus, the algorithm activates maximal numerical dissipation at the maximal sampling frequency of the element Ω_e^{max}, effectively dissipating the highest modes of the problem. So, when $\varphi_e^n \neq 0$, β_e^n assumes the following value:

$$\beta_e^{act} = (-\Omega_e^{max5} + 16\Omega_e^{max3} - 32\Omega_e^{max2}\zeta_e + 8(-\Omega_e^{max8}\zeta_e{}^2 - 16\Omega_e^{max6}\zeta_e{}^4 - 1024\Omega_e^{max4}\zeta_e{}^6 - 2\Omega_e^{max7}\zeta_e + 32\Omega_e^{max6}\zeta_e{}^2 - 96\Omega_e^{max5}\zeta_e{}^3 - 4096\Omega_e^{max3}\zeta_e{}^5 - \Omega_e^{max6} + 64\Omega_e^{max5}\zeta_e - 448\Omega_e^{max4}\zeta_e{}^2 + 1024\Omega_e^{max3}\zeta_e{}^3 - 6144\Omega_e^{max2}\zeta_e{}^4 + 32\Omega_e^{max4} - 672\Omega_e^{max3}\zeta_e + 3072\Omega_e^{max2}\zeta_e{}^2 - 4096\Omega_e^{max}\zeta_e{}^3 - 304\Omega_e^{max2} + 3072\Omega_e^{max}\zeta_e - 1024\zeta_e{}^2 + 1024)^{\frac{1}{2}} - 32\Omega_e^{max})/(\Omega_e^{max5} + 64\Omega_e^{max3}\zeta_e{}^2 + 128\Omega_e^{max2}\zeta_e + 64\Omega_e^{max}), \quad (4)$$

where $\zeta_e = \varsigma_e/(2\rho_e\omega_e^{max})$, and ω_e^{max}, ρ_e and ς_e stand for physical properties of the medium (maximum natural frequency, mass density and viscous damping coefficient, respectively). For $\varphi_e^n = 0$, $\beta_e^n = 0$ is considered.

3 Sub-cycling

Subcycling is a subdomain decomposition associated with multiple time-steps. This technique allows a domain to be discretized considering different refinement levels, without limiting the explicit analysis of time-marching restricted to its smallest critical time-step, which is commonly observed. The technique allows larger time-step values for different subdomains, resulting in lower computational costs. Despite allowing different time-step values for different subdomains, enabling lower computational costs, sub-cycling must be properly considered, once excessive subdivisions may provide deterioration in both accuracy and efficiency. Here, an automatic algorithm was developed to improve efficiency without compromising accuracy.

The following algorithm is considered to define the subdomain decomposition: (i) calculate the critical time-steps of all elements, finding the smallest Δt_e of the model (i.e., Δt_b, where $\Delta t_b = \min(\Delta t_e)$), which is the basic time-step for the controlled subdivision of the domain; (ii) with Δt_b defined, calculate subsequent time-step values as multiple of the power of 2 of this minimal time-step value (i.e., calculate Δt_i, where $\Delta t_i = 2^{(i-1)}\Delta t_b$); (iii) associate each element to a computed time-step value (i.e., to Δt_i, where $\Delta t_i \leq \Delta t_e \leq \Delta t_{i+1}$ and i indicates the subdomain of that element); (iv) associate a time-step value (i.e., associate a subdomain) to each degree of freedom of the model considering the lowest time-step value of its surrounding elements.

Once the subdomains of the model are stablished, displacement and velocity values along the boundaries of these subdomains may need to be interpolated. In this work, the following expressions are adopted for these interpolations:

$$\boldsymbol{U}(t) = \frac{1}{2\Delta t}\left(\dot{\boldsymbol{U}}^{n+1} - \dot{\boldsymbol{U}}^{n}\right)t^2 + \dot{\boldsymbol{U}}^{n}t + \boldsymbol{U}^{n}, \quad (5a)$$

$$\dot{\boldsymbol{U}}(t) = \frac{1}{\Delta t}\left(\dot{\boldsymbol{U}}^{n+1} - \dot{\boldsymbol{U}}^{n}\right)t + \dot{\boldsymbol{U}}^{n}, \quad (5b)$$

where t is the current increment of time ($0 \leq t \leq \Delta t$) for the focused subdomain and Δt is the time-step value of the degree of freedom being interpolated, which is related to another subdomain.

4 Numerical application

In this section, two numerical applications are considered to illustrate the performance and potentialities of the adaptive explicit time-marching technique with subcycling. First, it is considered a square homogeneous acoustic membrane, and, subsequently, the propagation of acoustic waves in the Marmousi2 model by Martin et al. [17] are analysed. The computed results are compared to those of the CDM, EG-α and β-adaptive method without subcycling. The EG-α [8] is considered here since it is a very well-known dissipative method. In the following analyses, lumped mass and damping matrices are always considered.

4.1 Application 1

In this application, the transverse motion of a square membrane, which has a unitary constant initial displacement prescribed over its central domain and null displacements prescribed over its entire boundary, is studied. The physical properties of the membrane are c = 10 m/s (wave velocity) and ρ = 1.0 kg/m3 (mass density). The model geometry is a square of side $L = 10\ m$, and the initial condition region is a centered square of side $l = 5\ m$. The symmetry of the membrane is considered and just 1/4 of it is discretized.

The membrane was discretized considering a concentration of elements along the boundary of the domain and the region of application of the initial condition, generating a mesh of 195944 linear triangular elements and 98525 nodes. This strategy was adopted because the application of the initial displacement generates a potential discontinuity, in addition, the analyzed degree of freedom (x=5, y=5) is also in this more refined area. Fig. 1a shows the Δt calculated to each element, resulting in three time-step subdomains, as shown in Fig. 1b. The active parameter values calculated for β with subcycling, are shown in the Fig. 1c.

This example has its analytical response known in the literature, which is given by:

$$u(x,y,t) = \frac{64A}{\pi^2}\sum_{m=1}^{\infty}\sum_{n=1}^{\infty}\frac{cos\ (\mu_{mn}t)}{mn}cos\left(\frac{m\pi}{4}\right)cos\left(\frac{n\pi}{4}\right)sin^2\left(\frac{m\pi}{4}\right)sin^2\left(\frac{n\pi}{4}\right)sin\left(\frac{m\pi x}{L}\right)sin\left(\frac{n\pi y}{L}\right), \quad (6)$$

where $\mu_{mn} = (c\pi/L)\left(m^2+n^2\right)^{\frac{1}{2}}$ and A is the amplitude of the applied initial displacement.

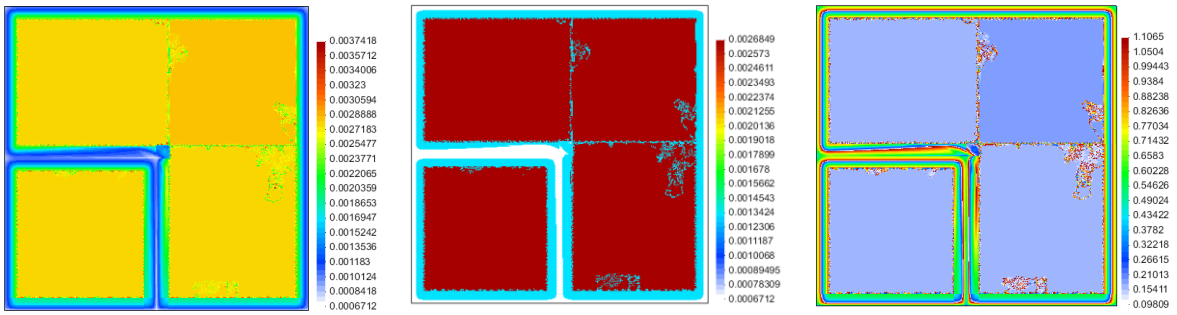

(a) (b) (c)

Figure 1. Subdomain decomposition and active β values for the first example (a) Δt for each element, (b) Δt for each subdomain, (c) active β values for the β-adap/sub.

In Fig. 2, time-history results for the transversal displacement are depicted, taking into account several time-marching procedures and the model's analytical response. As one can observe, the discussed time-marching procedure provides much more accurate results than standard techniques, and the effectiveness of this novel approach is improved once subcycling is applied. In fact, as one can notice, the discussed adaptive technique allows properly dissipating spurious numerical oscillations, providing much better responses than standard dissipative (e.g., the EG-α [8]) or non-dissipative (e.g., the CDM) approaches.

In Fig. 3, snap-shots of the results computed at time t = 1s, t=2s and t = 3s are depicted, considering the selected different time-marching techniques compared to the analytical answer. As can be observed, the CDM and EG-α do not provide appropriate results and spurious oscillations dominate the computed responses. On the other hand, good results are provided by the β-adap and β-adap/sub, illustrating their enhanced performance.

In Tab.1, the performance of each adopted technique is described. As one can observe, the β-adap/sub methodology provides the most accurate and efficient analyses (an Intel Core i7 -9750H 2.60GHz processor is considered for the analyses, with multiplications by the element stiffness matrices parallelized with OpenMP using 8 threads).

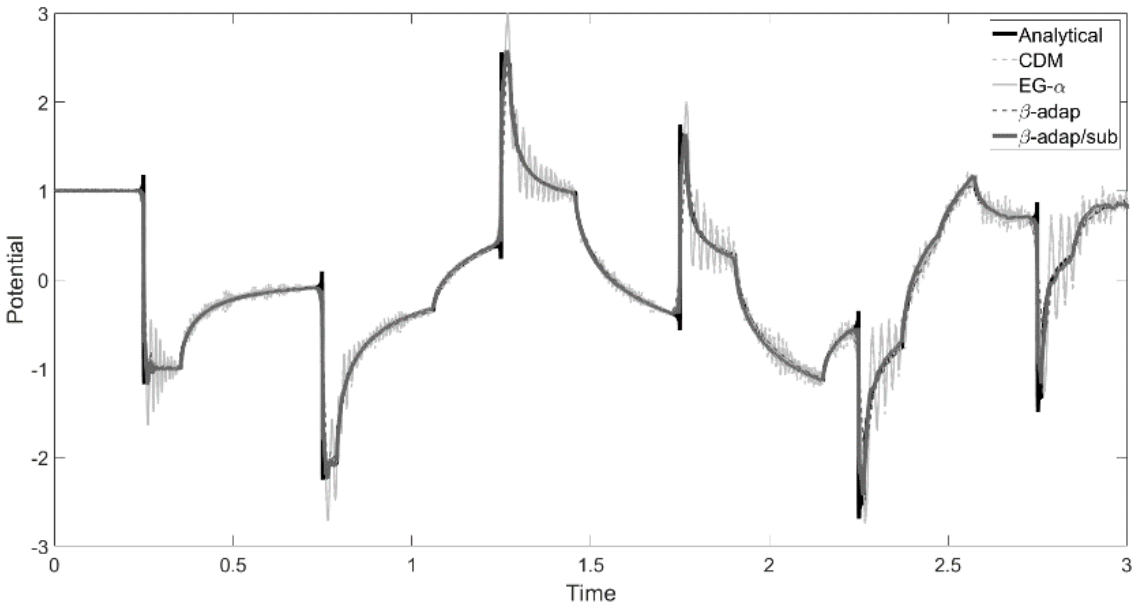

Figure 2. Time history results for the discussed time-marching procedures

Table 1. Performance of the analyses for the first example

Method	$\Delta t(10^{-3}\text{s})$	Steps	Error (10^{-1}) (relative error)	CPU Time (s) (relative time)
CDM	0.33560	8940	2.495 (1.47)	157.790 (3.45)
EG-α	0.30247	9919	2.420 (1.43)	171.720 (3.75)
β-adap	0.67121	4470	2.039 (1.20)	88.430 (1.93)
β-adap/sub	2.68486	1118	1.692 (1.00)	45.700 (1.00)

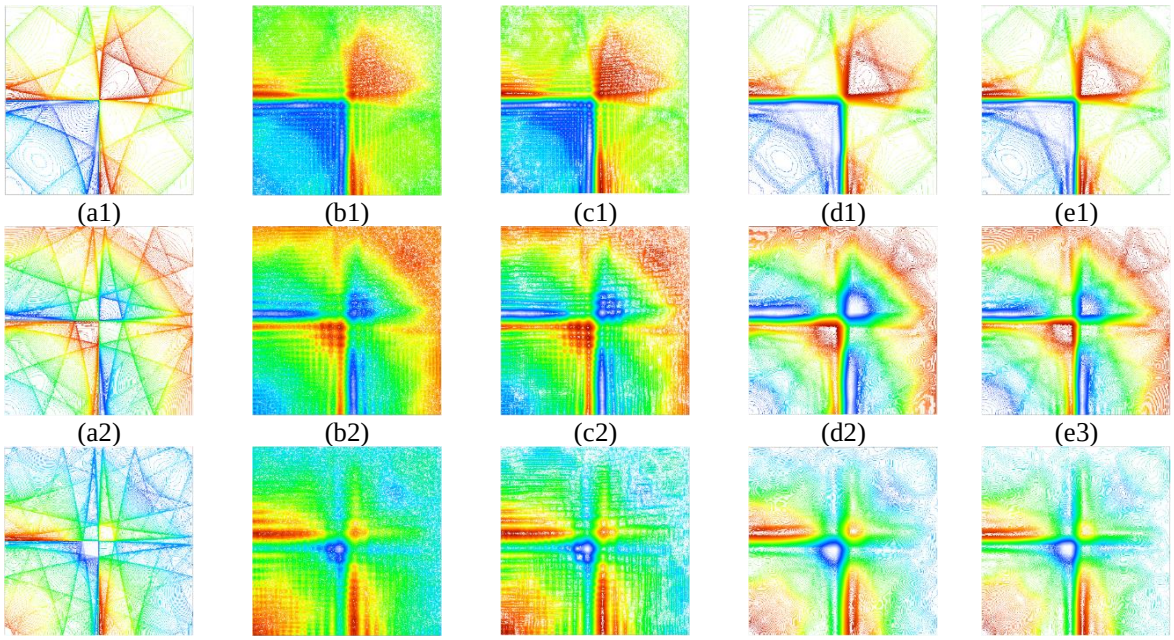

Figure 3. Computed fields along the discretized domain: (a) Exact solution, (b) CDM, (c) EG-α, (d) β-adap and (e) β-adap/sub at (1) 1s, (2) 2s and (3) 3s

4.2 Application 2

In this second example, an extension of the original Marmousi2 model created by Martin et al. [17] is analysed. The model has a lateral extension of 17 km and a depth of 3.5 km and includes a total of 199 geological layers, as well as an extended water layer of 450 m deep. Here, the original finite difference synthetic data are transformed into a FEM mesh with 224731 nodes and 223672 linear square elements. Thus, just the wave propagation velocity of each material controls the variability of the element time-steps. In Fig.4, the obtained subdomain decomposition and active β values are depicted.

Fig. 5 shows the computed fields along the model, taking into account the selected solution procedures, and Table 2 describes the performance of the analyses. As can be seen, the subdomain decomposition and subcycling techniques performed well for this complex heterogeneous model, allowing the evaluation of precise solutions at lower computational costs.

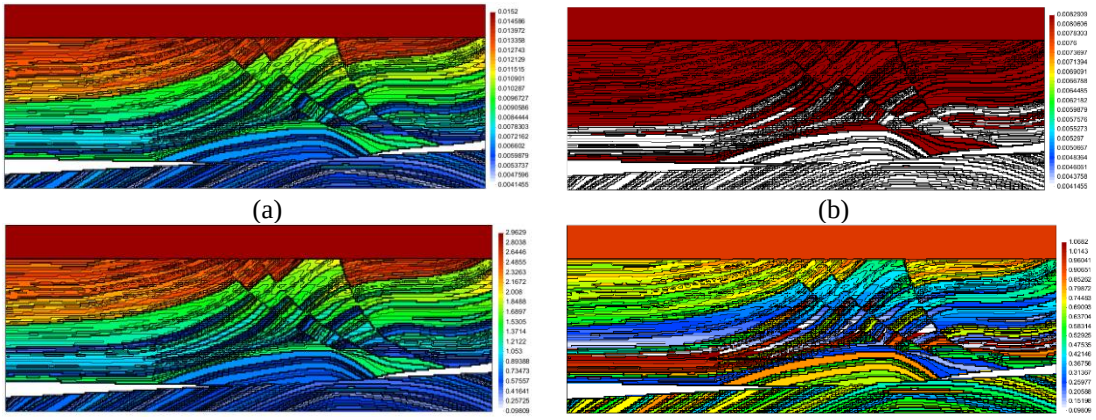

(a) (b) (c) (d)

Figure 4. Subdomain decomposition and active β values for the second example: (a) Δt for each element, (b) Δt for each subdomain, (c) active β values for the β-adap and (d) active β values for the β-adap/sub.

Table 2. Performance of the analyses for the second example

Method	$\Delta t(10^{-3}\text{s})$	Steps	CPU Time (s) (relative time)
CDM	2.0727	700	40.210 (2.22)
EG-α	1.8680	780	47.520 (2.63)
β-adap	4.1455	350	24.300 (1.34)
β-adap/sub	8.2909	175	18.080 (1.00)

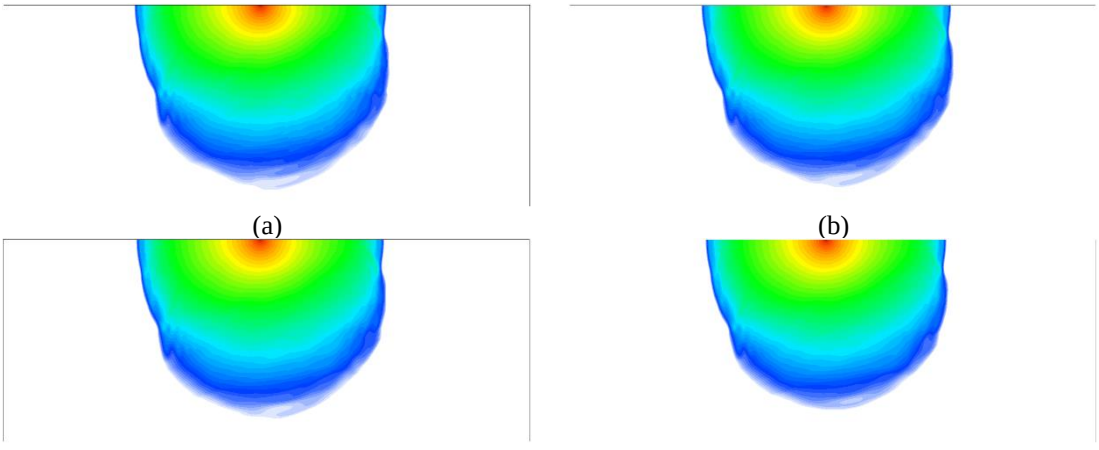

(a) (b) (c) (d)

Figure 5. Computed fields along the discretized domain:(a) CDM, (b) EG-α, (c) β-adap and (d) β-adap/sub at t=1.4s

5 Conclusions

In this paper an explicit fully adaptive time-marching formulation for hyperbolic models is presented, in which both the time-step and time integrator values adapt to the properties of the discretized model, allowing to provide a more efficient and accurate solution methodology. This methodology is applied with the subcycling technique, which allows better calculations of time-step values. In this work, two acoustic examples are discussed to illustrate the good performance of the proposed approach. As the examples demonstrate, the proposed formulation allows to obtain better results than standard solution procedures, considering less computational efforts. In the second example, a complex heterogeneous model is studied, highlighting the robustness of the proposed automated formulation.

Acknowledgements. The financial support by CNPq (Conselho Nacional de Desenvolvimento Científico e Tecnológico), CAPES (Coordenação de Aperfeiçoamento de Pessoal de Nível Superior), FAPEMIG (Fundação de Amparo à Pesquisa do Estado de Minas Gerais), PRH-ANP (Programa de Recursos Humanos da Agência Nacional do Petróleo, Gás Natural e Biocombustíveis) and PETROBRAS (CENPES – 21066) is greatly acknowledged.

References

[1] Soares Jr, D. (2020). A novel time-marching formulation for wave propagation analysis: the adaptive hybrid explicit method. *Computer Methods in Applied Mechanics and Engineering*, 366, 113095.
[2] Soares Jr, D. (2021). A multi-level explicit time-marching procedure for structural dynamics and wave propagation models. *Computer Methods in Applied Mechanics and Engineering*, 375, 113647.
[3] Zhang, H. M., & Xing, Y. F. (2019). Two novel explicit time integration methods based on displacement-velocity relations for structural dynamics. *Computers & Structures*, 221, 127-141.
[4] Noh, G., & Bathe, K. J. (2013). An explicit time integration scheme for the analysis of wave propagations. *Computers & structures*, 129, 178-193.
[5] Kim, W. (2019). An accurate two-stage explicit time integration scheme for structural dynamics and various dynamic problems. International Journal for Numerical Methods in Engineering, 120(1), 1-28.
[6]Soares Jr, D. (2020). Efficient high-order accurate explicit time-marching procedures for dynamic analyses. Engineering with Computers, 1-15.
[7] Soares Jr, D. (2019). An adaptive semi-explicit / explicit time marching technique for nonlinear dynamics. *Computer Methods in Applied Mechanics and Engineering*, 354, 637-662.
[8] Hulbert, G. M., & Chung, J. (1996). Explicit time integration algorithms for structural dynamics with optimal numerical dissipation. *Computer Methods in Applied Mechanics and Engineering*, 137(2), 175-188.
[9] Soares Jr, D. (2019). A model/solution-adaptive explicit-implicit time-marching technique for wave propagation analysis. International Journal for Numerical Methods in Engineering, 119(7), 590-617.
[10] Hilber, H. M., Hughes, T. J., & Taylor, R. L. (1977). Improved numerical dissipation for time integration algorithms in structural dynamics. *Earthquake Engineering & Structural Dynamics*, 5(3), 283-292.
[11] Wood, W. L., Bossak, M., & Zienkiewicz, O. C. (1980). An alpha modification of Newmark's method. *International journal for numerical methods in engineering*, 15(10), 1562-1566.
[12] Newmark, N. M. (1959). A method of computation for structural dynamics. *Journal of the engineering mechanics division*, 85(3), 67-94.
[13] Soares Jr, D. (2015). A simple and effective new family of time marching procedures for dynamics. *Computer Methods in Applied Mechanics and Engineering*, 283, 1138-1166.
[14] Bathe, K. J., & Baig, M. M. I. (2005). On a composite implicit time integration procedure for nonlinear dynamics. *Computers & Structures*, 83(31-32), 2513-2524.
[15] Chung, J., & Hulbert, G. M. (1993). A time integration algorithm for structural dynamics with improved numerical dissipation: the generalized-α method. *Journal of Applied Mechanics*, 60(2): 371-375.
[16] Tamma, K. K., Zhou, X., & Sha, D. (2000). The time dimension: a theory towards the evolution, classification, characterization and design of computational algorithms for transient / dynamic applications. *Archives of Computational Methods in Engineering*, 7(2), 67-290.
[17] Martin, G. S., Wiley, R., & Marfurt, K. J., 2006. Marmousi2: An elastic upgrade for marmousi. *The leading edge*, vol. 25, n. 2, pp. 156–166.